IEEE Access
Multidisciplinary | Rapid Review | Open Access Journal

Received September 2, 2020, accepted September 16, 2020, date of publication September 28, 2020,
date of current version October 8, 2020.

Digital Object Identifier 10.1109/ACCESS.2020.3027045

Matched-Phase Weighting Beamformer to Improve the Gain of a Long Linear Array in the Range-Dependent Ocean Waveguide

LEI XIE[1], CHAO SUN[2], (Member, IEEE), AND DEZHI KONG[2]
[1]College of Oceanic and Atmospheric Sciences, Ocean University of China, Qingdao 266100, China
[2]School of Marine Science and Technology, Northwestern Polytechnical University, Xi'an 710072, China

Corresponding author: Chao Sun (csun@nwpu.edu.cn)

This work was supported by the National Natural Science Foundation of China under Grant 11534009 and Grant 11904342.

ABSTRACT The array gain degrades significantly suffering from a decrease of signal spatial coherence caused by imperfectly correlated acoustic channels with spatial and temporal fluctuations. For a long linear array collecting signals in the range-dependent ocean waveguide, the amplitude and phase of the received signals show more viriation over the elements, which causes the signal coherence to attenuate seriously. The gain of traditional beamformers, such as the conventional beamformer (CBF), minimum variance distortionless response beamformer (MVDR-BF), and eigenvalue beamformer (EBF), will deviate from their ideal values. In this paper, a matched-phase weighting beamformer (MPBF) is proposed to obtain high gain in an ocean waveguide. The variational phase of acoustic channel transfer functions over the elements can be compensated for by matched-phase weighting, and then, the acoustic channel spatial coherence can be restored to achieve a high gain. The weighting-matrix of MPBF is obtained by the received signals; hence, environmental parameters or channel transfer functions do not have to be estimated. Simulations and experiments considering a long horizontal uniform linear array (HLA) in the slope region receiving a narrow-band signal from a deep-water source (upslope waveguide) are performed. The results demonstrate that MPBF can achieve a higher gain than CBF, MVDR-BF and EBF in a complex ocean waveguide.

INDEX TERMS Array gain, ocean waveguide, spatial coherence, matched-phase weighting.

I. INTRODUCTION

A long linear array has a great advantage in detecting weak signals from underwater targets. One of the major factors is that a long linear array can achieve a high array gain (AG) by using a beamformer on the receiving data. AG is defined as the improvement in the signal-to-ratio (SNR) at the output of beamforming compared with the input SNR. AG depends on the sum of the correlation coefficients between all pairs of elements of the array, for both the noise and signal [1]. Under ideal assumptions, such as the noise between two arbitrary elements being uncorrelated and the signal having perfect plane wave (far field) or spherical wave arrivals (near field), AG can have the ideal value of $10\log_{10} M$, where M is number of elements in the array. However, both of the assumptions in the mathematical model are violated in sonar signal processing in the ocean waveguide. The real ocean waveguide always manifests as a complex acoustic channel with spatial and temporal fluctuations subject to the topography and acoustic properties of the sea-floor, as well as eddies, tides, internal wave, and surface gravity waves [2]. The coherence of the signal on two spatially separated elements will decrease [3]–[5], after the sound wave propagates through imperfectly correlated acoustic channels. Moreover, in the continental slope area, the variation of an acoustic channel introduced by the range-dependent waveguide is more serious. In this case, AGs of traditional beamformers, such as the conventional beamformer (CBF), the minimum variance distortionless response beamformer (MVDR-BF) [6], and the eigenvalue beamformer (EBF) [7], [8], deviate from the ideal value. For a long linear array, AG will no longer increase after the number of elements reaches a certain value, which is the limiting gain [9]. Ultimately, the advantages of using a long linear array to detect targets will be greatly

The associate editor coordinating the review of this manuscript and approving it for publication was Mohammad Zia Ur Rahman.

weakened or the targets will not be able to be successfully detected.

To weaken the impact of the multipath arrival on AG, two representative beamforming methods based on the acoustic field model are proposed: the matched-field beamform [10] and the matched-mode beamform [11]. Both methods try to use the information of the sound field and waveguide environment to optimize the output of the processor. Hence, these processes require the hydrological parameters of the ocean waveguide and an accurate model of sound field to accurately calculate the replica vector. For the range-dependent waveguide, however, the replica fields have to be updated regularly to maintain a high gain [12]. The accuracy and speed of the acoustic field calculated are often not guaranteed due to the complex changes of hydrological and seabed parameters. In addition, the coupled modes in the range-dependent waveguide makes it difficult to extract modes, and matched-mode processing is difficult to realize. A number of studies have discussed the effects of coherence attenuation on AG [13]–[15], and subarray processing is provided to achieve a higher AG. Green gave the optimum number of subarrays for a given length array considering the linear and exponential decay of coherence [16]. However, the subarray division needs to predict the signal coherence length. In addition, this process attenuates the gain of the whole array, which weakens the advantage of the detection using a long linear array. Some researchers have developed a method based on the linear phase relationship of the waveguide invariance to improve the acoustic channel coherence to obtain a higher AG [17]. In the range-dependent waveguide, the frequency-phase-shift between the frequency response functions at two received positions is not linear with horizontal separation. Hence, this method is not effective for a range-dependent waveguide.

Sound waves transferring in the range-dependent ocean waveguide is neither a plane wave nor a perfect match to a multipath mode, caused by the variational acoustic channels. Previous research has investigated the effect of phase fluctuations on AG in the stochastic ocean [18], [19]. Based on this understanding, we have derived the analytical expression of the AG of a uniform linear array (ULA) using acoustic channel transfer functions. The theoretical analysis demonstrates that AG will be close to the ideal value, if the difference between two arbitrary Δ s values (Δ is the phase difference between the channel transfer function and the weight coefficient of the element) approximates $2n\pi$ (where n is a integer), in which case all the received signals are phase congruent [20]. In other words, the acoustic channels at two arbitrary elements after weighting are completely correlated, and AG can achieve the ideal value. Taking CBF as an example, the weighting phase of CBF will compensate for the phase difference if the phase difference between two adjacent acoustic channels is constant, i.e., it is a phase-matched weighting. However, in the range-dependent ocean waveguide, the received signals have nonuniform amplitude/phase (the phase difference is not constant) over the elements and the signal coherence decreases with element separation. In this case, the conventional method is unable to compensate for the phase difference. Actually the conventional weighting is a kind of phase mismatched weighting. This paper introduces a matched-phase beamformer (MPBF) that utilizes the phase differences between the signal at the reference element and those at the other elements in the array to design complex weighting coefficients. MPBF can compensate for the phase of acoustic channels and improve acoustic channel coherence to obtain a high gain. Both the simulation and experimental results for a low-frequency narrowband signal propagating in the upslope waveguide indicate that the MPBF has a higher gain than the CBF, MVDR-BF and EBF.

The remainder of this paper is divided into four sections. Section II outlines the beamformers based on the plane waves and the influence of wavefront distortion or correlation attenuation on AG. The mechanism of the gain attenuation in the ocean waveguide is given in Section III. On this basis, the matched-phase weighting method and the MPBF are proposed. In Section IV, AG is calculated as a function of the element number utilizing numerical simulations and the experimental data collected by a long horizontal uniform linear array (HLA) in the South China Sea. Comparing the performances of CBF, MVDR-BF, EBF and MPBF, the results demonstrate that MPBF can restore acoustic channel coherence and improve AG in the range-dependent ocean waveguide. Finally, we provide a short summary and draw conclusions in Section V.

II. ARRAY GAIN FOR PLANE WAVE

Array gain is defined as

$$ag = \frac{SNR_{\text{array}}}{SNR_{\text{hyp}}}, \tag{1}$$

where SNR_{array} is the SNR at the array output, and SNR_{hyp} is that at a single element. For a beamformer, AG can be obtained as follows [21]

$$ag = \frac{\left|\sum_{i=1}^{M} w_i s_i\right|^2}{\sum_{i=1}^{M} |s_i|^2} \Bigg/ \frac{\left|\sum_{i=1}^{M} w_i n_i\right|^2}{\sum_{i=1}^{M} |n_i|^2}, \tag{2}$$

where w_i is the weighting coefficient of the i th element, and s_i and n_i are the signal and noise at the i th element, respectively. Assuming the ambient noise is uncorrelated and the noise powers on the elements are equal, AG can be simplified as

$$ag = M\left|\sum_{i=1}^{M} w_i s_i\right|^2 \Bigg/ \sum_{i=1}^{M} |w_i|^2 \sum_{i=1}^{M} |s_i|^2, \tag{3}$$

One can infer from (3) that the optimal weight coefficients (reaching the ideal gain) make $w_i s_i$ on each element accumulate coherently. We take three representative beamformers (CBF, MVDR-BF, EBF) for ULA as examples to investigate the influence of weight mismatching on AG.

The weighting coefficient of CBF at the i th element is

$$w_{\text{CBF},i} = \exp\left[-j2\pi f(i-1)d\cos\vartheta/c\right], \tag{4}$$

where f is the signal frequency, c is the sound speed of in the seawater, d is the spacing between two adjacent elements in the array, and ϑ is the direction of signal arrival (measured from the endfire of the array). The weighting amplitude is uniform, $|w_{\mathrm{CBF},i}| = 1/M$.

The weighting vector of the MVDR-BF is

$$\boldsymbol{w}_{\text{MVDR-BF}} = \frac{\boldsymbol{R}^{-1}\boldsymbol{a}(\vartheta)}{\boldsymbol{a}^{H}(\vartheta)\boldsymbol{R}^{-1}\boldsymbol{a}(\vartheta)}, \tag{5}$$

where $\boldsymbol{R}$ is the covariance matrix of the array receiving data and $\boldsymbol{a}(\vartheta)$ is the array steering vector. The constraint of no distortion implies that $|\boldsymbol{w}_{\text{MVDR-BF}}|^2 = 1$.

The weighting vector of the EBF is obtained by eigen-decomposition of the signal covariance matrix $\boldsymbol{R}_s$

$$\lambda_i \boldsymbol{e}_i = \boldsymbol{R}_s \boldsymbol{e}_i, \quad i = 1, 2, \ldots r = \mathrm{rank}(\boldsymbol{R}_s), \tag{6}$$

where λ_i and $\mathbf{e}_i$ are the i th eigenvalue and the corresponding eigenvector, respectively. The eigenvector corresponding to the largest eigenvalue is taken as the weighting vector $\boldsymbol{w}_{\text{EBF}}$, and $|\boldsymbol{w}_{\text{EBF}}|^2 = 1$.

The gains of the CBF and MVDR-BF can be calculated according to (3), respectively, as follows

$$\begin{aligned} ag_{\text{CBF}} &= M^2 \left| \sum_{i=1}^{M} w_{\text{CBF},i} s_i \right|^2 \Big/ \sum_{i=1}^{M} |s_i|^2 \\ ag_{\text{MVDR-BF}} &= M \left| \sum_{i=1}^{M} w_{\text{MVDR-BF},i} s_i \right|^2 \Big/ \sum_{i=1}^{M} |s_i|^2. \end{aligned} \tag{7}$$

It is clear from (5) and (6) that the weights of the CBF and MVDR-BF are related to the angle of the incoming wave. In free space, the sound wave reaches the array as plane wave with a determined arrival angle, and the time-delay (time domain) or phase difference (frequency domain) between two adjacent acoustic channels is constant, i.e., the acoustic channels are completely correlated. The signals on all elements can accumulate coherently after weighting (as (7)) to obtain the ideal gain. However, for a sound wave propagated in a nonuniform waveguide, the wavefront is distorted, or the signal arrives as multipath. In this case, the weight phases of the CBF and MVDR-BF are mismatched, and AG deviates from the ideal value.

Assuming that the ambient noise is uncorrelated, the gain of EBF is determined by the ratio of $\lambda_{\max}$ to the sum of all eigenvalues [8],

$$ag_{\text{EBF}} = \frac{M\lambda_{\max}\boldsymbol{w}_{\text{EBF}}^{H}\boldsymbol{w}_{\text{EBF}}}{\boldsymbol{w}_{\text{EBF}}^{H}\boldsymbol{w}_{\text{EBF}}\mathrm{Tr}(\boldsymbol{R}_s)} = \frac{M\lambda_{\max}}{\sum_{i=1}^{M}\lambda_i}, \tag{8}$$

The symbol $\mathrm{Tr}(\cdot)$ denotes the matrix trace. Equation (8) seems to be not affected by the wavefront distortion. However, the coherence attenuation due to the ocean waveguide will change the distribution of the eigenvalues [13], as demonstrated by the decrease of the ratio of the largest eigenvalue and the sum of all eigenvalues. Ultimately, the gain of the EBF is less than the ideal value.

We have outlined the performances of the CBF, MVDR-BF and EBF, thus demonstrating that AGs are affected by wavefront distortion or coherence attenuation. The above three beamformers have poor performances in processing the signals after propagating in a complex ocean waveguide, especially for a wide-aperture array. Indeed, the purpose of the time delays or phase shifts that can be introduced into the array for steering is to compensate for the phase differences between acoustic channels. One can estimate Green's functions of the ocean waveguide to match the phases of the acoustic channels [22]. However, this estimation is difficult to conduct in the range-dependent waveguide, and the its accuracy may not work for phase matching. In practice, the phases of the acoustic channels are not necessary, but the phase differences between all pairs of acoustic channels are determinant in beamforming. In the following, we present the mechanism by which the nonuniform amplitude and phase of acoustic channel transfer functions affect AG. On this basis, we propose the matched-phase weighting method, which is valid for compensating the phase variation of the acoustic channel transfer function and enhancing the spatial coherence of acoustic channels to obtain a higher gain in the inhomogeneous ocean waveguide.

III. MATCHED PHASE BEAMFORMING

A. ARRAY GAIN IN AN OCEAN WAVEGUIDE

The ocean waveguide has different impacts on the signal field and the noise field, and the elements in the array have different outputs. We take the average of the SNRs at all elements as the single element reference required in the definition of (1) and divide AG into signal gain and noise gain [23],

$$ag = \frac{SNR_{\text{array}}}{SNR_{\text{average}}} = \frac{S_{\text{array}}}{S_{\text{average}}} \Big/ \frac{N_{\text{array}}}{N_{\text{average}}} = \frac{asg}{ang}, \tag{9}$$

where

S_{array} is the signal power of the array output,
S_{average} is the average signal power of all elements,
N_{array} is the noise power of the array output,
N_{average} is the average noise power of all elements,
asg is the array signal gain: $asg = S_{\text{array}}/S_{\text{average}}$,
ang is the array noise gain: $ang = N_{\text{array}}/N_{\text{average}}$.

Assuming that the ambient noise is isotropic, ang has been derived in [24]

$$ang = \sum_{i=1}^{M} w_i^2 + 2\sum_{i=1}^{M-1}\sum_{k=i+1}^{M} w_i w_j^* \frac{\sin[2\pi(i-k)d/\lambda]}{2\pi(i-k)d/\lambda}, \tag{10}$$

where the superscript "$*$" denotes the complex conjugate operation. From (10), when $d = \lambda/2$, $ang = \sum_{i=1}^{M} w_i^2$. We are only concerned with this special case in this paper.

The propagation of sound waves in the ocean waveguide is described by the wave equations that can be solved using different models, such as the normal mode, ray, direct finite-difference and parabolic equations [25]. For a short-duration pulse, the acoustic channel can be regarded as linear time-invariant and characterized by the channel

impulse response $h(t)$ in the time domain or the transfer function $H(f)$ in the frequency domain. The receiving signal in the frequency domain at the i th element can be described as

$$S_i(f) = X(f)H_i(f), \tag{11}$$

where $X(f)$ is the source spectrum and $H_i(f)$ is the acoustic channel transfer function between the source and the i th element at frequency f.

We derived the expression of AG with uniform weighting amplitude via the acoustic channel transfer functions as [20]

$$ag = \frac{\left|\sum_{i=1}^{M} A_i \exp(-j\psi_i)\exp(j\theta_i)\right|^2}{\sum_{i=1}^{M}|A_i|^2} = \frac{\left|\sum_{i=1}^{M} A_i \exp(j\Delta_i)\right|^2}{\sum_{i=1}^{M}|A_i|^2}, \tag{12}$$

where A_i and ψ_i are the amplitude and the phase of $H_i(f)$, respectively; θ_i is the phase of the weighting coefficient; and Δ_i is the phase difference between the channel transfer function and the weight coefficient of the i th element, i.e., $\Delta_i = \theta_i - \psi_i$. It has been demonstrated that the non-uniform amplitude of the acoustic channel transfer function has a slight effect on AG; however, the phase mismatch is a major factor that leads AG to further deviate from its ideal value. Hence, the weighting amplitude can be uniform, and a suitable weighting phase should be designed to compensate for the phase of the channel transfer function.

According to (12), AG will be close to the ideal value if $\theta_i = \psi_i$ or $\Delta_i = 0$ for all elements, i.e., the weighting phases are matched with those of the channel transfer functions. However, for a passive sonar system, ψ_i is difficult to estimate by the received signal since the signals have been modulated by the acoustic channels (as in (11)) which have spatial and temporal fluctuations.

We can expand (12) utilizing the Euler formula, $\exp(j\Delta_i) = \cos(\Delta_i) + j\sin(\Delta_i)$, as

$$ag = \left|\sum_{i=1}^{M} A_i\cos(\Delta_i)\right|^2 + \left|\sum_{i=1}^{M} A_i\sin(\Delta_i)\right|^2 \Bigg/ \sum_{i=1}^{M}|A_i|^2, \tag{13}$$

to further investigate the influence of the weighting phase. After some manipulations, we obtain the expression of AG as,

$$ag = \sum_{i=1}^{M}\sum_{k=1}^{M} A_iA_k\cos(\Delta_i - \Delta_k) \Bigg/ \sum_{i=1}^{M}|A_i|^2. \tag{14}$$

From (14), we can infer that the matched phase condition will be satisfied if $\Delta_i - \Delta_k = 0$ for all elements. Switching "$\Delta_i - \Delta_k = 0$" as

$$\Delta_i - \Delta_k = (\theta_i - \psi_i) - (\theta_k - \psi_k) = (\theta_i - \theta_k) - (\psi_i - \psi_k) = 0. \tag{15}$$

we can see that a higher gain is obtained when the phase difference of the weighting coefficients on two arbitrary elements is equal to the phase difference of the transfer functions on the corresponding elements. According to the theoretical result discussed above, we can design the weighting coefficient of the MPBF.

B. MATCHED-PHASE WEIGHTING METHOD

According to (11), we can obtain the phase difference of the acoustic channel transfer functions on two elements,

$$\psi_i - \psi_k = \text{angle}\left[H_i(f)H_k(f)^*\right] = \text{angle}\left[S_i(f)S_k(f)^*\right]. \tag{16}$$

We take the element at the front-end of the array as a reference and set the weighting phase on the reference element to 0. According to (15) and (16), we can design the weight phase on the i th element as

$$\theta_i(f) = \psi_i - \psi_0 = \text{angle}\left[S_i(f)S_0(f)^*\right], \tag{17}$$

where $S_i(f)$ and $S_0(f)$ are the receiving signals (in the frequency domain) on the i th element and the reference element, respectively.

Using the uniform weighting amplitude, the weight coefficient on the i th element is written as by its phase

$$w_{\text{MP}}(i) = \frac{1}{M}\exp\left[j\theta_i(f)\right], \tag{18}$$

The subscript MP denotes matched-phase. We demonstrate that the variational phases of the acoustic channel transfer functions over different elements in the array can be compensated for by this method.

We assume that the phase weighting on the reference element is θ_0, i.e., $\theta_0(f) = 0$ and the phase of the corresponding acoustic channel transfer function is $\psi_0(f)$. Then, the phases of weighting coefficients on the i th and k th element can be obtained, respectively,

$$\begin{aligned}\theta_i(f) &= \psi_i(f) - \psi_0(f) = \text{angle}\left[S_i(f)S_0(f)^*\right]\\ \theta_k(f) &= \psi_k(f) - \psi_0(f) = \text{angle}\left[S_k(f)S_0(f)^*\right],\end{aligned} \tag{19}$$

Therefore, the phase difference between the weighting coefficient and the transfer function on the i th element is

$$\Delta_i = \theta_i(f) - \psi_i(f) = \psi_i(f) - \psi_0(f) - \psi_i(f) = -\psi_0(f). \tag{20}$$

Similarly, the phase difference of the reference element and the k th element can be calculated, respectively, as follows

$$\begin{aligned}\Delta_0 &= \theta_0(f) - \psi_0(f) = -\psi_0(f)\\ \Delta_k &= \theta_k(f) - \psi_k(f) = -\psi_0(f).\end{aligned} \tag{21}$$

From (20) and (21), we can observe that the matched-phase weighting method using (17) and (18) enables the phase difference Δ between two arbitrary elements in the array to be equal to $-\psi_0(f)$. As a consequence,

$$\Delta_{ik} = \Delta_i - \Delta_k = -\psi_0(f) + \psi_0(f) = 0. \tag{22}$$

This approach satisfies the condition that the difference of Δ is equal to 0; thus, a higher gain can be obtained.

We have demonstrated how to implement matched-phase weighting and proved that the weight phases obtained by

(17) and (18) are valid to compensate for the variational phase of the channel transfer functions. Generally, received signals have a certain bandwidth. In this case, the weight vector of a single in-band frequency is first obtained by this method, and then the weight vectors of all the frequencies in the bandwidth can be formed into a weighting matrix for beamforming. In the following section, we apply the phase matching approach to the narrow-band signal, and propose the corresponding beamforming method MPBF.

C. MATCHED-PHASE BEAMFORMING FOR A NARROW-BAND SIGNAL

We assume that the array receives a narrow-band signal with frequencies from f_{L} to f_{H}. First, the fast Fourier transform (FFT) is applied to the received data of each element, and the spectra can be obtained and the frequency bins in the narrow-band is Q. Then, we can obtain the weight coefficients at the frequency in the narrow-band $[f_{\mathrm{L}}, f_{\mathrm{H}}]$, according to (17) and (18). Finally, the weight matrix of the MPBF can be obtained by composing the weight vectors at all frequencies,

$$\boldsymbol{W}_{\mathrm{MP}} = \begin{bmatrix} w_{\mathrm{MP}}(1,f_1) & \cdots & w_{\mathrm{MP}}(1,f_q) & \cdots & w_{\mathrm{MP}}(1,f_Q) \\ \vdots & & \vdots & & \vdots \\ w_{\mathrm{MP}}(i,f_1) & \cdots & w_{\mathrm{MP}}(i,f_q) & \cdots & w_{\mathrm{MP}}(M,f_Q) \\ \vdots & & \vdots & & \vdots \\ w_{\mathrm{MP}}(M,f_1) & \cdots & w_{\mathrm{MP}}(M,f_q) & \cdots & w_{\mathrm{MP}}(M,f_Q) \end{bmatrix}^{\mathrm{T}}, \tag{23}$$

where the superscript "T" denotes the transpose operation. The matched-phase weight on the i th element is

$$\begin{aligned} w_{\mathrm{MP}}(i,f_q) &= \frac{1}{M}\exp\left(j\theta_i(f_q)\right), \quad f_q \in [f_L, f_H] \\ w_{\mathrm{MP}}(i,f_q) &= 1/M, \quad f_q \notin [f_L, f_H] \\ \theta_i\left(f_q\right) &= \mathrm{angle}\left[S_i(f_q)S_0(f_q)^*\right], \end{aligned} \tag{24}$$

where $S_i(f_q)$ and $S_0(f_q)$ are the spectra of the received signal by the i th element and the reference element at the frequency f_q, respectively. The weighting phases on the reference element are set to 0, i.e., $w_{\mathrm{MP}}(1,f) = 1$.

In the passive sonar detection, the received data usually contain a noise component. One can use the received data to obtain the weight matrix $\boldsymbol{W}_{\mathrm{MP}}$. Assuming the signal and noise are uncorrelated, the spectrum of the received data on the i th element $\boldsymbol{P}_i$ is

$$\boldsymbol{P}_i = \boldsymbol{S}_i + \boldsymbol{N}_i, \tag{25}$$

where $\boldsymbol{S}_i$ and $\boldsymbol{N}_i$ are the spectrum of the signal and noise, respectively. Equation (24) can be rewritten as

$$\begin{aligned} w_{\mathrm{MP}}(i,f_q) &= \frac{1}{M}\exp\left(j\theta_i(f_q)\right), \quad f_q \in [f_L, f_H] \\ w_{\mathrm{MP}}(i,f_q) &= 1/M, \quad f_q \notin [f_L, f_H] \\ \theta_i\left(f_q\right) &= \mathrm{angle}\left[P_i(f_q)P_0(f_q)^*\right], \end{aligned} \tag{26}$$

where $P_i(f_q)$ and $P_0(f_q)$ are the spectra of the data on the i th element and the reference element at frequency f_q, respectively.

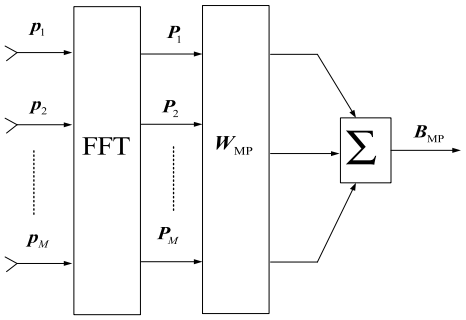

FIGURE 1. Flow chart of the MPBF.

The outputs of all elements weighted by $\boldsymbol{W}_{\mathrm{MP}}$ are summed to obtain the output of the MPBF,

$$\boldsymbol{B}_{\mathrm{MP}} = \sum_{i=1}^{M} (\boldsymbol{W}_{\mathrm{MP}} \circ \boldsymbol{P}_i), \tag{27}$$

where the symbol "$\circ$" represents the Hadamard product.

Based on the above analysis, the flowchart of the MPBF can be obtained, as shown in Fig. 1.

In summary, the MPBF algorithm can be implemented in three steps:

1. Apply the FFT operation to the data and obtain $\boldsymbol{P}$;
2. Calculate $\boldsymbol{W}_{\mathrm{MP}}$ according to (26);
3. Obtain the beam output of $\boldsymbol{B}_{\mathrm{MP}}$ by summing all the data on the elements after weighting by $\boldsymbol{W}_{\mathrm{MP}}$, as given in (27).

According to the definition of AG in (9), the gain of MPBF is

$$ag_{\mathrm{MPBF}} = \frac{\left|\sum_{i=1}^{M} \boldsymbol{S}_{\mathrm{MP},i}\right|^2}{\left|\sum_{i=1}^{M} \boldsymbol{N}_{\mathrm{MP},i}\right|^2} \Big/ \frac{\sum_{i=1}^{M} |\boldsymbol{S}_i|^2}{\sum_{i=1}^{M} |\boldsymbol{N}_i|^2}, \tag{28}$$

where $\boldsymbol{S}_{\mathrm{MP}}$ and $\boldsymbol{N}_{\mathrm{MP}}$ are the beam output of the signal and noise on the i th element, respectively, after weighting by phase matching

$$\begin{aligned} \boldsymbol{S}_{\mathrm{MP},i} &= \boldsymbol{W}_{\mathrm{MP},i} \circ \boldsymbol{S}_i \\ \boldsymbol{N}_{\mathrm{MP},i} &= \boldsymbol{W}_{\mathrm{MP},i} \circ \boldsymbol{N}_i. \end{aligned} \tag{29}$$

In the following section, we verify the performance of the MPBF using the simulation and experimental data of HLA in the upslope waveguide. Comparative analysis of the AGs for various processors are conducted to verify that MPBF has a higher gain in the upslope ocean waveguide.

IV. SIMULATION

The ocean geometry in the continental slope (range-dependent ocean waveguide) is illustrated in Fig. 2. The whole area can be divided into three different regions: an abyssal plain, a continental slope area, and shallow water. The abyssal plain extends for 2 km with a water depth of 5000 m. Assuming that the oblique angle of the slope is 3.5°, the continental slope covers a range from 2 km to 90 km with the water depth varying from 5000 m to 229 m. Finally, a 20 km distance in shallow water is considered with a depth of 229 m, making the whole distance in the three regions 100 km in

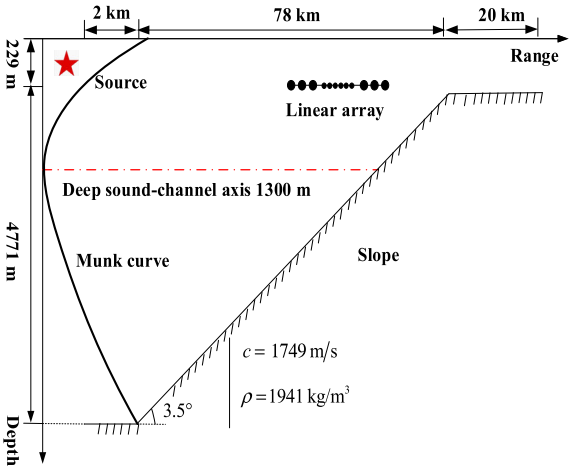

FIGURE 2. Simulation environment and parameters.

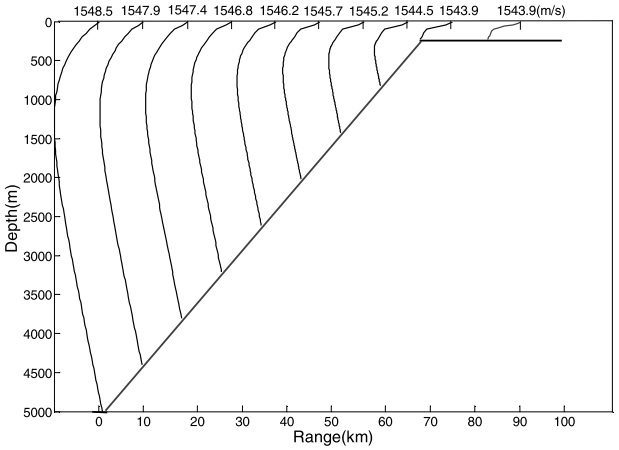

FIGURE 3. Sound speed profiles of the upslope waveguide at 10 km intervals.

the simulations. The bottom absorption coefficients for all three regions are assumed to be the same 0.5 dB/λ. Assuming that the sound speed profile (SSP) of the shallow water has a negative gradient speed profile and that the SSP of the abyssal sea is a standard Munk curve with a deep sound channel axial at 1300 m, the SSPs of the continental slope region are presented every 10km, as shown in Fig. 3.

The source is at a fixed depth of 550 m, radiating a narrow-band signal with a center frequency of 190Hz. An HLA with 100 elements ($M = 100$) is suspended in the slope region at a depth of 120 m. The spacing between adjacent elements is 4 m, approximately equal to half the wavelength corresponding to 190 Hz. The acoustic channel transfer functions are obtained by the RAM program based on the split-step Padé algorithm for the parabolic equation [26]. The average SNR at the elements is −10 dB. Taking the receiving distance of 30 km as an example, we first compare the acoustic channel coherence before and after weighting by the MPBF. And then, the gain of the MPBF is compared with that of the CBF, MVDR-BF and EBF.

A. ACOUSTIC CHANNEL SPATIAL COHERENCE

The spatial correlation coefficient of the acoustic channels at the i th and the k th elements is calculated in frequency

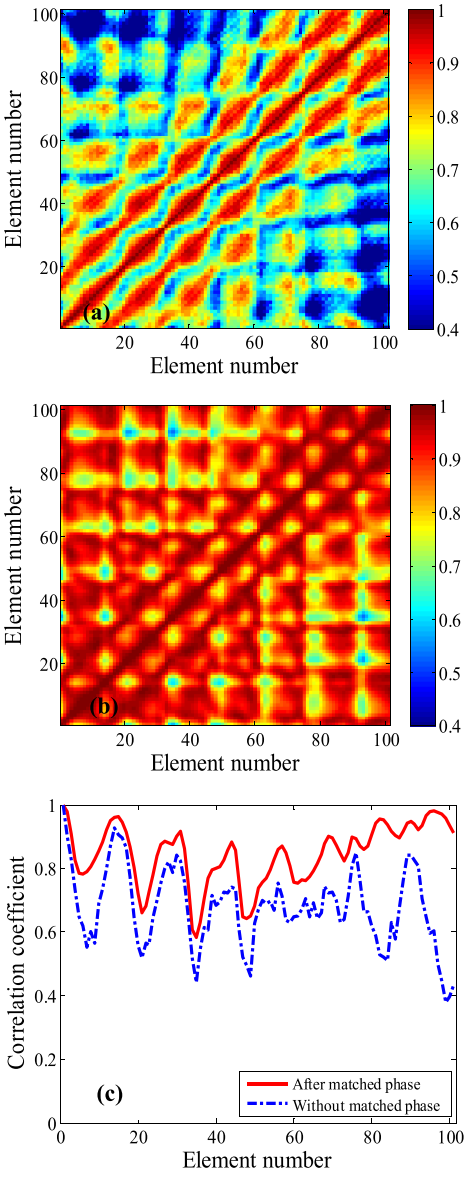

FIGURE 4. Correlation coefficients of the acoustic channels in the upslope waveguide: (a) and (b) results without and with matched-phase weighting, respectively; (c) the correlation coefficients between the reference element and the other elements without (blue dash-dotted line) and after matched-phase weighting (red solid line). The source is at a depth of 550 m, and the HLA is 30 km away from the source at a depth of 120 m.

domain as [17]

$$\rho_{ik} = \max_{\tau} \left\{ \frac{\mathrm{Re}\left[\int_{f_L}^{f_H} H_i(f) H_k(f)^* e^{j2\pi f \tau} df\right]}{\sqrt{\int_{f_L}^{f_H} |H_i(f)|^2 df} \sqrt{\int_{f_L}^{f_H} |H_k(f)|^2 df}} \right\}, \quad (30)$$

where τ is the time compensation and $\mathrm{Re}[\cdot]$ represents taking the real part. At a receiving distance of 30 km, the correlation coefficients between all pairs of elements are shown in Fig. 4(a). The correlation coefficients decrease with the increase of element spacing and then present an oscillating downtrend, due to the multipath propagation manifested as the nonuniform amplitude and phase of the channel transfer functions. This outcome ultimately leads to the gains

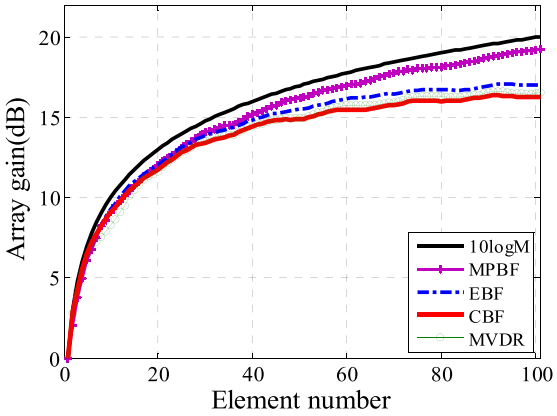

FIGURE 5. Simulated array gains with the number of elements for the CBF (red solid line), MVDR-BF (green solid line with "○"), EBF (blue dash-dotted line) and MPBF (purple solid line with "+"), respectively.

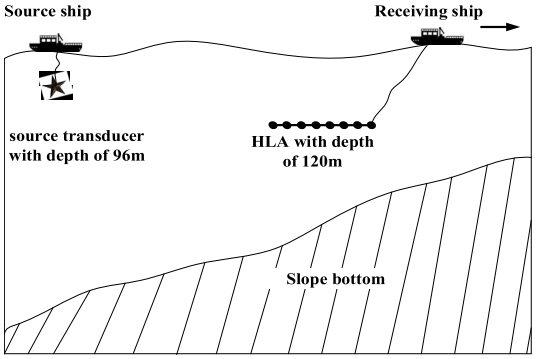

FIGURE 6. Source-receiver configuration of experiment.

of the CBF, MVDR-BF and EBF being lower than the ideal value.

Utilizing the received data of the HLA, $\boldsymbol{W}_{\mathrm{MP}}$ is obtained according to (26), and the correlation coefficients are calculated after a matched-phase operation. Fig. 4(b) shows the correlation coefficients between all pairs of elements. All the correlation coefficients are greater than 0.7, although the coherence is still attenuated. In comparison, the correlation coefficients between the reference and other elements in the HLA are shown in Fig. 4(c), including the correlation coefficients after matched-phase weighting. The sum of all the correlation coefficients in Fig. 4(c) is 67.59 (the mean value is 0.6759), yet the sum is 84.41 (the mean value is 0.8441) after matched-phase weighting. It is clear from Fig. 4 that the correlation coefficients with matched-phase weighting are greater than those without it, which verifies that the phase variation of the channel transfer functions can be compensated for by the matched-phase weighting method, and then, the acoustic channel coherence can be significantly improved.

B. THE GAINS OF VARIOUS BEAMFORMERS

According to (9), the gains of the four kinds of beamformers at a distance of 30 km are calculated as a function of element number, as shown in Fig. 5. In contrast, the solid black line in Fig. 5 shows the ideal value of AG, i.e., $10\log_{10} M$. We can observe that the gains of the CBF (red solid line), MVDR-BF (green solid line with "○"), EBF (blue dash-dotted line) and MPBF (purple solid line with "+") are the same and equal to the ideal value when the number of elements is less than 7. Then, the gains of the four kinds of beamformers increase with the number of elements, but all of them are less than the ideal value, due to the degradation of acoustic channel coherence. The gain of the MPBF starts to be larger than that of the other three beamformers when the number of elements reaches 40 (the array length is 156 m). In addition, when the number of elements reaches 75(the array length is 296 m), the gains of the three traditional beamformers almost no longer increase with the number of elements, but the gain of the MPBF continues to increase. For the whole HLA with 100 elements, the gains of the CBF, MVDR-BF, EBF and MPBF are 16.27 dB, 16.54 dB, 17.03 dB and 19.23 dB, respectively. The gain of the MPBF is significantly higher than that of the other three beamformers and close to the ideal value of 20 dB.

The acoustic channel coherence and performances of the CBF, MVDR-BF and EBF and MPBF are simulated when the long HLA operates in the upslope waveguide. The results show that the acoustic channels are affected by the ocean waveguide, leading to the degradation of coherence. The gains of the CBF, MVDR-BF and EBF deviate from the ideal value and do not increase with the number of elements if the element number reaches a certain value. However, the matched-phase weighting method compensates for the phase variation of the acoustic channel transfer function, improves the coherence, and finally, can obtain a higher gain. Next, we verify the performance of the MPBF utilizing experimental data collected by a long HLA in the northwest of the South China Sea.

V. EXPERIMENT RESULT

A. EXPERIMENTAL REVIEW

The experiment was carried out using two ships in the South China Sea in July 2014. The source ship maintained its position in shallow water, and the source transducer was suspended at a normal depth of 96 m, radiating a pseudo-random signal with frequencies from 50 Hz to 360 Hz. The signal was transmitted twice every 1210 s with a duration of 1200 s and propagated through an upslope waveguide. A long HLA (receiving array) was towed by the receiving ship away from the fixed source ship at a speed of 4.4 knots. The array had 192 elements uniformly spaced at 1.5 m, and the sampling frequency was 12 kHz. We chose the collected data when the array was 24 km away from the source and towed at a depth of 120 m. Fig. 6 and 7 show the source-receiver configuration and the station diagram in the experiment, respectively.

The following analysis requires confidence that there is no interference signal in the received data and that the SNR is relatively high. First, we operate a narrow-band filter with a frequency from 115 Hz to 125 Hz on each element, and a narrow band signal with a central frequency 120 Hz

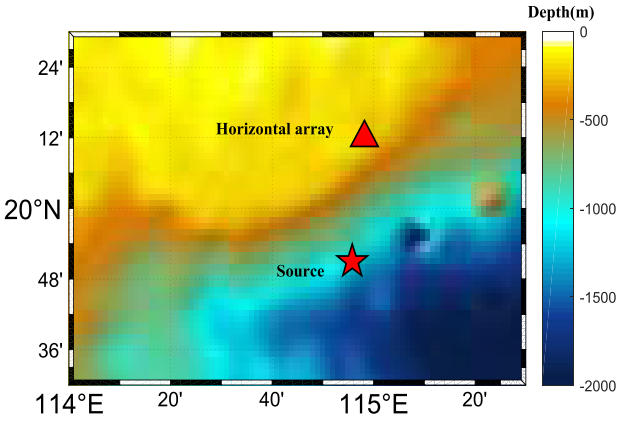

FIGURE 7. Station diagram of the source and the HLA.

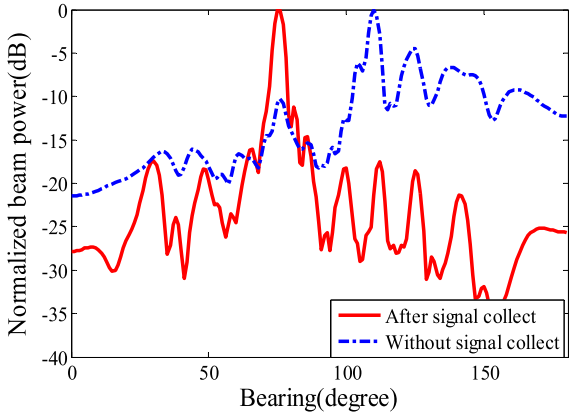

FIGURE 8. CBF swept-beam analysis using signals without (blue dash-dotted line) and after signal collection (red solid line), respectively.

(bandwidth 10 Hz) is obtained. Then, the towed array is divided into several subarrays overlapping each other, and the optimum beamforming is carried out for each subarray to improve the SNR of the received data and suppress interference. The subarray output is taken as the signal on the element at the front-end of the subarray. In this paper, the subarray has 20 elements, and the number of elements overlapping adjacent subarrays is 19. For the HLA with 192 elements, the received signals of 172 elements can be obtained, and the spacing between adjacent elements in the array is also 1.5 m. The data from the 10th to the 110th elements are chosen to analyze the signal collected. The beam powers of the CBF (as an example) are shown in Fig. 8 using data without (blue dash-dotted line) and after signal collection (red solid line). The bearing of the target is 76° measured from the end-fire of the array. It is found that the signal power is almost 13 dB higher than the noise power, and the interferences (at 110°, 125° and 138°) are suppressed. Finally, the received data are obtained by adding the Gaussian noise with equal power on each element. The average SNR is −10 dB, the same as the simulation. We investigate the acoustic channel coherence and the performances of the CBF, MVDR-BF, EBF and MPBF using the data after signal collection.

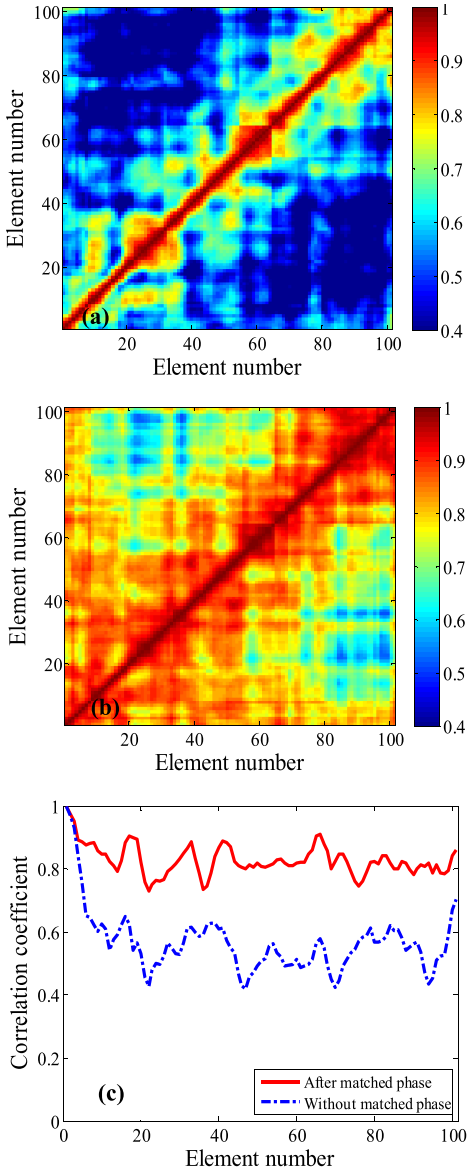

FIGURE 9. Correlation coefficients of signals in the experiment: (a) and (b) results without and with matched-phase weighting, respectively; (c) correlation coefficients between the reference element and the other element without (blue dash-dotted line) and after matched-phase weighting (red solid line). The source is at a depth of 96 m, and the HLA is 24 km away from the source at a depth of 120 m.

B. SIGNAL SPATIAL COHERENCE

Generally, the acoustic channel correlation coefficient can be a measure of the corresponding signal coherence [27]. In the experiment, it is difficult to estimate the acoustic channel transfer function accurately. Here, we calculate the signals coherence instead of the spatial coherence of the acoustic channel transfer functions. Following the analysis in the simulation, the correlation coefficients between all pairs of signals are calculated, as shown in Fig. 9. We observe that the coherence rapidly decreases with the increase of element spacing, as shown in Fig. 9(a).

The weight matrix of matched-phase $\boldsymbol{W}_{\mathrm{MP}}$ is obtained according to (26). The signal correlation coefficients after

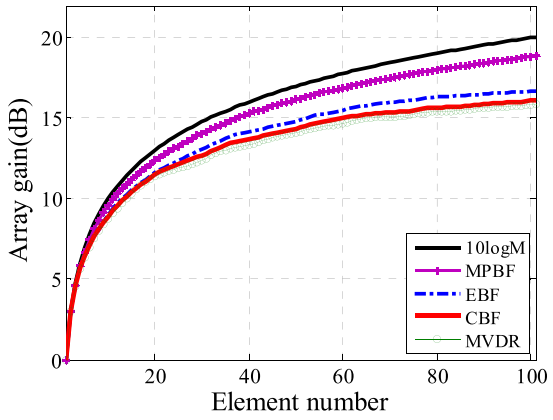

FIGURE 10. Array gains with the number of elements for the CBF (red solid line), MVDR-BF (green solid line with "○"), EBF (blue dash-dotted line) and MPBF (purple solid line with "+"), respectively.

matched-phase weighting are shown in Fig. 9(b) which shows that the correlation coefficients are almost greater than 0.7. For comparative analysis, Fig. 9(c) shows the correlation coefficients between the reference element and the other element in the HLA before and after the matched-phase weighting. The sum of all the correlation coefficients without matched-phase weighting is 57.09 (the blue dots draw lines), yet the sum is 83.59 (the red solid line) after matched-phase weighting. It is clear that the signal coherence can be improved (the acoustic channel coherence be restored), after compensating for the phase of the channel transfer function by the matched-phase weighting method with a uniform amplitude weighting.

C. THE GAINS OF VARIOUS BEAMFORMERS

From Fig. 9., we can be speculated that the gains of the CBF, MVDR-BF and EBF will be less than the ideal value, due to the degradation of the signal coherence. According to (9), we calculate the gains of the four kinds of beamformers as functions of the element number, as shown in Fig. 10. One can observe that the gains of the CBF, MVDR-BF, EBF and MPBF are equal to the ideal value when the number of elements is less than 5. Then, the gains increase with the number of elements but reach less than the ideal value. The gains of the CBF and MVDR-BF are approximately equal but less than the gains of EBF when the number of elements exceeds 20. When the number of elements reaches 7 (the array length is 9 m), the gain of the MPBF starts to exceed that of the other three beamformers. For the HLA with 100 elements, the gains of the CBF, MVDR-BF, EBF and MPBF are 16.10 dB, 15.85 dB, 16.68 dB and 18.81 dB, respectively. It is clear that the gain of the MPBF is significantly higher than that of the three traditional beamformers. Hence, the MPBF can be expected a high gain in the real ocean waveguide.

VI. SUMMARY AND CONCLUSION

The mechanism of array gain degradation caused by the imperfectly correlated acoustic channels in the range-dependent ocean waveguide is studied, based on which the MPBF is proposed to improve AG. The performance of the MPBF has been investigated using simulated and experimental data received by a long HLA in the upslope waveguide. The results of the acoustic channel coherence and the corresponding AG are presented as a function of the element number (or array length).

The acoustic channel is affected by the nonuniform ocean waveguide, which leads to the distortion of the wavefront or multipath arrival. For the plane-wave beamformers (CBF, MVDR-BF, EBF), the weighting phase cannot compensate for the phase of the acoustic channel, i.e., phase mismatch. The phase mismatch is the major factor that results in the decrease of AG. Assuming the ambient noise is isotropic, the analytical expression of AG considering the acoustic channel is derived as (14), which shows the influence of the phase difference (Δ) between the weighting phase and channel transfer function phase on AG. This finding indicates that AG will be close to the ideal value if the difference between two arbitrary Δs approximates $2n\pi$ (n is an arbitrary integer). Based on the above analysis, the matched-phase method is proposed. The phase difference between two acoustic channel transfer functions can be extracted using the received data in the frequency domain. And then, the matched-phase beamforming can be carried out using this phase difference as the weighting phase.

Numerical simulation and experimental data of a long HLA in the upslope waveguide are processed. First, the acoustic channel correlation coefficients without and after matched-phase weighting are calculated, as shown in Fig. 4 and 9. These figures demonstrate that the correlation coefficients after the matched-phase weighting are greater than 0.7, which verifies that matched-phase weighting can compensate for the phase of the acoustic channel transfer function and restore the acoustic channel coherence. Then, the performances of the CBF, MVDR-BF, EBF and MPBF are compared with the data received by the HLA. The gains of four kinds beamformer are calculated as a function of the element number, as shown in Fig. 5 and 10. The gains of the three traditional beamformers increase with the number of elements when the number of elements is small (the array length is short enough). However, the gains do not increase further when the number of elements exceeds a certain value, which is caused by the attenuation of the acoustic channel coherence. The gain of the MPBF is larger than that of the CBF, MVDR-BF and EBF and close to the ideal value, $10\log_{10} M$. Both the results of the simulation and experiment demonstrate that the MPBF can avoid the decrease of AG caused by imperfectly correlated acoustic channels in the range-dependent ocean waveguide.

Overall, this research demonstrates a new beamforming method, termed matched-phase weighting beamforming, that can obtain a high gain in a complex ocean waveguide. Based on the phase matching with the acoustic channel transfer functions, the MPBF overcomes the influence of imperfectly correlated acoustic channels on the array output. Additionally, the received data usually contain a noise

component; hence, the extraction of the phase difference between channel transfer functions is subject to the SNR of the data.

REFERENCES

[1] R. J. Urick, *Principles of Underwater Sound*, 3rd ed. Westport, CT, USA: Peninsula Publishing, 1983, p. 33.
[2] J. A. Colosi, *Sound Propagation Through the Stochastic Ocean*, 1st ed. Cambridge, U.K.: Cambridge Univ. Press, 2016, pp. 6–12.
[3] W. M. Carey, "The determination of signal coherence length based on signal coherence and gain measurements in deep and shallow water," *J. Acoust. Soc. Amer.*, vol. 104, no. 2, pp. 831–842, 1998.
[4] T. F. Duda, J. M. Collis, Y.-T. Lin, and J. F. Lynch, "Observed intensity and horizontal field coherence variability of low-frequency pulse transmissions on the continental shelf," *J. Acoust. Soc. Amer.*, vol. 124, no. 4, p. 2442, 2008.
[5] L. Wan and M. Badiey, "Horizontal coherence of sound propagation in the presence of internal waves on the New Jersey continental shelf," *J. Acoust. Soc. Amer.*, vol. 137, no. 4, p. 2390, 2015.
[6] J. Capon, "High-resolution frequency-wavenumber spectrum analysis," *Proc. IEEE*, vol. 57, no. 8, pp. 1408–1418, Aug. 1969.
[7] J.-L. Yu and C.-C. Yeh, "Generalized eigenspace-based beamformers," *IEEE Trans. Signal Process.*, vol. 43, no. 11, pp. 2453–2461, Nov. 1995.
[8] C.-C. Lee and J.-H. Lee, "Eigenspace-based adaptive array beamforming with robust capabilities," *IEEE Trans. Antennas Propag.*, vol. 45, no. 12, pp. 1711–1716, Dec. 1997.
[9] H. Cox, "Line array performance when the signal coherence is spatially dependent," *J. Acoust. Soc. Amer.*, vol. 54, no. 6, pp. 1743–1746, Dec. 1973.
[10] A. B. Baggeroer, W. A. Kuperman, and P. N. Mikhalevsky, "An overview of matched field methods in ocean acoustics," *IEEE J. Ocean. Eng.*, vol. 18, no. 4, pp. 401–424, Oct. 1993.
[11] T. C. Yang, "Effectiveness of mode filtering: A comparison of matched-field and matched-mode processing," *J. Acoust. Soc. Amer.*, vol. 87, no. 5, pp. 2072–2084, May 1990.
[12] M. H. Orr and P. C. Mignerey, "Matched-field processing gain degradation caused by tidal flow over continental shelf bathymetry," *J. Acoust. Soc. Amer.*, vol. 111, no. 6, pp. 2615–2621, 2002.
[13] K. D. Heaney, "Shallow water narrowband coherence measurements in the florida strait," *J. Acoust. Soc. Amer.*, vol. 129, no. 4, pp. 2026–2041, Apr. 2011.
[14] E. Y. Gorodetskaya, A. I. Malekhanov, A. G. Sazontov, and N. K. Vdovicheva, "Deep-water acoustic coherence at long ranges: Theoretical prediction and effects on large-array signal processing," *IEEE J. Ocean. Eng.*, vol. 24, no. 2, pp. 156–171, Apr. 1999.
[15] M. Orr, B. Pasewark, S. Wolf, J. Lynch, and C.-S. Chiu, "Bottomed acoustic array gain variability in the South China Sea," *J. Acoust. Soc. Amer.*, vol. 114, no. 4, p. 2460, 2003.
[16] M. C. Green, "Gain of a linear array for spatially dependent signal coherence," *J. Acoust. Soc. Amer.*, vol. 60, no. 1, pp. 129–132, Jul. 1976.
[17] Y. Zhang, F. Li, and X. Su, "Improvement of longitudinal correlation of explosive signals by using waveguide invariance," *J. Acoust. Soc. Amer.*, vol. 1272, no. 1, pp. 454–461, 2010.
[18] R. A. Wagstaff, "The Wagstaff's integration silencing processor filter: A method for exploiting fluctuations to achieve improved sonar signal processor performance," *J. Acoust. Soc. Amer.*, vol. 104, no. 5, pp. 2915–2924, Nov. 1998.
[19] R. A. Wagstaff, "Exploiting phase fluctuations to improve temporal coherence," *IEEE J. Ocean. Eng.*, vol. 29, no. 2, pp. 498–510, Apr. 2004.
[20] L. Xie, C. Sun, G.-Y. Jiang, X.-H. Liu, and D.-Z. Kong, "Effect of the fluctuant acoustic channel on the gain of a linear array in the ocean waveguide," *Chin. Phys. B*, vol. 27, no. 11, Nov. 2018, Art. no. 114301.
[21] H. L. Van Trees, *Optimum Array Processing: Detection, Estimation, and Modulation Theory*, 1st ed. New York, NY, USA: Wiley, 2002, pp. 63–66.
[22] K. G. Sabra and D. R. Dowling, "Blind deconvolution in ocean waveguides using artificial time reversal," *J. Acoust. Soc. Amer.*, vol. 116, no. 1, pp. 261–271, 2004.
[23] R. M. Hamson, "The theoretical gain limitations of a passive vertical line array in shallow water," *J. Acoust. Soc. Amer.*, vol. 68, no. 1, pp. 156–164, Jul. 1980.
[24] M. J. Buckingham, "Array gain of a broadside vertical line array in shallow water," *J. Acoust. Soc. Amer.*, vol. 65, no. 1, pp. 148–161, Jan. 1979.
[25] F. B. Jensen, W. A. Kuperman, and M. B. Porter, *Computational Ocean Acoustics*, 2nd ed. Springer, 2011.
[26] M. D. Collins, "A split-step Padé solution for the parabolic equation method," *J. Acoust. Soc. Amer.*, vol. 93, no. 4, pp. 1736–1742, Apr. 1993.
[27] W. M. Carey and W. B. Moseley, "Space-time processing, environmental-acoustic effects," *IEEE J. Ocean. Eng.*, vol. 16, no. 3, pp. 285–301, Jul. 1991.

LEI XIE received the B.S. degree in information technology and the Ph.D. degree in underwater acoustic engineering from the School of Marine Science and Technology, Northwestern Polytechnical University (NWPU), Xi'an, China, in 2011 and 2018, respectively. He is currently pursuing his postdoctoral research with the College of Oceanic and Atmospheric Sciences, Ocean University of China, Qingdao, China. His research interests include underwater sound propagation, the effects of internal wave, and array signal processing.

CHAO SUN (Member, IEEE) received the B.S. degree in applied electronics from Northwestern Polytechnical University (NPU), Xi'an, China, in 1986, and the Ph.D. degree in electronics and electrical engineering from Loughborough University, Loughborough, U.K., in 1992. Since 1992, she has been with the School of Marine Science and Technology, NPU, where she is currently a Full Professor. From 2000 to 2001, she was a Visiting Research Fellow of the Marine Physical Laboratory, University of California San Diego, San Diego, CA, USA. Her research interests include array signal processing, underwater acoustic signal processing, parameter estimation, and adaptive techniques. She was the Chairperson of the Underwater Acoustics Chapter of the Acoustical Society of China from 2005 to 2013 and is currently a member of the Acoustical Society of America.

DEZHI KONG received the B.E. degree in information technology from Northwestern Polytechnical University, Xi'an, China, in 2014, where he is currently pursuing the Ph.D. degree in under water acoustic engineering. His current research interests include signal detection and adaptive processing with applications to under water environment.